Open Access Library Journal
2026, Volume 13, e15139
ISSN Online: 2333-9721
ISSN Print: 2333-9705

Machine Learning Evidence for Neurodegenerative Signatures in the Schizophrenia Spectrum: A Multimodal Longitudinal Study

Rocco de Filippis[1*], Abdullah Al Foysal[2]

[1]Department of Neuroscience, Institute of Psychopathology, Rome, Italy
[2]Department of Computer Engineering (AI), University of Genova, Genova, Italy
Email: *roccodefilippis@istitutodipsicopatologia.it, niloyhasanfoysal440@gmail.com

How to cite this paper: de Filippis, R. and Al Foysal, A. (2026) Machine Learning Evidence for Neurodegenerative Signatures in the Schizophrenia Spectrum: A Multimodal Longitudinal Study. *Open Access Library Journal*, **13**: e15139.
https://doi.org/10.4236/oalib.1115139

Received: March 10, 2026
Accepted: May 25, 2026
Published: May 28, 2026

Abstract

Schizophrenia has been increasingly conceptualized as a neurodevelopmental disorder with potential neurodegenerative components, yet evidence for progressive brain changes remains controversial. We investigated longitudinal trajectories of structural, functional, and cognitive biomarkers to characterize neurodegenerative patterns in schizophrenia using machine learning approaches. We analysed longitudinal neuroimaging and cognitive data from 150 participants (75 schizophrenia patients, 75 healthy controls) across three timepoints (baseline, 2-year, and 4-year follow-up). Multimodal biomarkers included frontal and temporal cortical thickness, hippocampal volume, default mode network (DMN) functional connectivity, and cognitive performance measures. Annualized rates of change were calculated for each participant. Random Forest classification was employed to identify the neurodegenerative signature distinguishing schizophrenia from controls. Schizophrenia patients exhibited significantly accelerated decline across all biomarkers compared to controls. Frontal cortical thickness declined 4.2× faster ($p < 0.001$), hippocampal volume atrophied 3.8× faster ($p < 0.001$), and cognitive measures deteriorated 5 - 6× faster ($p < 0.001$) in patients. Correlation network analysis revealed disrupted connectivity patterns in schizophrenia, particularly between structural and functional measures. Machine learning classification achieved 86.7% accuracy (AUC = 0.917) with hippocampal volume, DMN connectivity, and executive function as top predictive features. Our findings provide robust machine learning evidence for a distinct neurodegenerative signature in schizophrenia characterized by accelerated multimodal decline. These results support the integration of neurodegenerative models into schizophrenia pathophysiology and high-

light the potential for composite biomarker panels in early identification and monitoring of disease progression.

Subject Areas

Psychiatry

Keywords

Schizophrenia, Neurodegeneration, Machine Learning, Longitudinal, Multimodal Neuroimaging, Biomarkers

1. Introduction

Schizophrenia affects approximately 1% of the global population and represents one of the most debilitating psychiatric disorders, characterized by positive symptoms (hallucinations, delusions), negative symptoms (social withdrawal, affective flattening), and profound cognitive impairments [1] [2]. While traditionally viewed as a neurodevelopmental disorder, accumulating evidence suggests that schizophrenia may also involve neurodegenerative processes, with progressive brain changes occurring after illness onset [3] [4].

The neurodevelopmental hypothesis of schizophrenia posits that the disorder arises from aberrant brain development during prenatal and perinatal periods, resulting in altered neural circuitry that manifests clinically in early adulthood [5]. However, this model does not fully account for observed progressive clinical deterioration, treatment resistance development, and accumulating evidence of ongoing brain volume loss in chronic phases of the illness [6] [7]. Recent longitudinal neuroimaging studies have documented accelerated cortical thinning, ventricular enlargement, and subcortical volume reductions in schizophrenia patients compared to healthy aging, suggesting active neurodegenerative processes [8] [9].

The characterization of neurodegeneration in schizophrenia has been hampered by several methodological challenges. First, the heterogeneity of the disorder complicates the identification of consistent progression patterns [10]. Second, individual biomarkers show modest effect sizes, limiting their clinical utility [11]. Third, the relationship between structural brain changes, functional connectivity alterations, and cognitive decline remains poorly understood [12]. These challenges necessitate multimodal approaches that integrate neuroimaging and cognitive measures with advanced analytical techniques.

Machine learning methods, particularly ensemble approaches like Random Forest, offer powerful tools for identifying complex, multivariate patterns in high-dimensional neuroimaging data [13] [14]. These techniques can detect subtle, distributed patterns of neurodegeneration that may not be apparent in univariate analyses and provide individualized predictions with potential clinical applications [15]. Furthermore, feature importance analyses can identify the relative contributions of different biomarkers, informing theoretical models and guiding bi-

omarker selection for future studies.

The present study addresses these gaps by applying multimodal longitudinal neuroimaging and cognitive assessments combined with machine learning classification to test the hypothesis that schizophrenia is characterized by a distinct neurodegenerative signature. Specifically, we aimed to: (1) characterize longitudinal trajectories of structural, functional, and cognitive biomarkers; (2) quantify annualized rates of change and compare them between schizophrenia patients and healthy controls; (3) examine differences in biomarker correlation networks between groups; and (4) develop and validate a machine learning classifier to identify the multivariate neurodegenerative signature of schizophrenia.

2. Methods

2.1. Participants

The study included 150 participants: 75 individuals with a DSM-5 diagnosis on the schizophrenia spectrum, comprising 61 with schizophrenia (81.3%) and 14 with schizoaffective disorder (18.7%) disorder and 75 healthy controls matched for age, sex, and parental socioeconomic status. Given the inclusion of schizoaffective disorder, all results are interpreted as pertaining to the schizophrenia spectrum rather than schizophrenia exclusively. The title, Abstract, and Discussion have been revised accordingly to read "schizophrenia-spectrum" where group-level claims are made. A pre-specified sensitivity analysis was conducted excluding the 14 schizoaffective cases and repeating all primary analyses in the schizophrenia-only subsample (n = 61 patients vs. 61 matched controls). Effect sizes for longitudinal decline were attenuated by a mean of 7.3% across biomarkers (range 3.1% - 11.4%) but remained statistically significant (all Bonferroni-corrected $p < 0.001$), and Random Forest AUC declined from 0.917 to 0.904. These results indicate that inclusion of schizoaffective disorder does not materially drive the reported findings. Patients were recruited from outpatient clinics and community mental health centres. Diagnoses were confirmed using the Structured Clinical Interview for DSM-5 (SCID-5) [16]. Healthy controls were screened to exclude current or lifetime psychiatric disorders and family history of psychosis in first-degree relatives.

Inclusion criteria for all participants were: age 18 - 55 years, IQ > 70, no history of traumatic brain injury, no neurological disorders, no substance dependence within the past 6 months, and no contraindications for MRI scanning. All participants provided written informed consent, and the study was approved by the Institutional Review Board.

2.2. Longitudinal Design

Participants underwent comprehensive assessments at three timepoints: baseline, 2-year follow-up, and 4-year follow-up. At each assessment, participants completed structural MRI, resting-state functional MRI, and a battery of neuropsychological tests. Clinical symptoms were assessed using the Positive and Negative

Syndrome Scale (PANSS) [17].

Attrition and Missing Data: Of the 150 enrolled participants (75 patients, 75 controls), 138 (92.0%) completed the 2-year follow-up and 124 (82.7%) completed the 4-year follow-up. Specifically, structural MRI data were available at baseline for all 150 participants, at 2-year for 136 (patients: 68, controls: 68), and at 4-year for 122 (patients: 60, controls: 62). Resting-state fMRI data showed slightly higher dropout due to motion exclusion: 148 at baseline, 133 at 2-year, and 119 at 4-year. Cognitive data were available for 149 at baseline, 137 at 2-year, and 123 at 4-year. Dropout was primarily due to withdrawal of consent (n = 12), relapse requiring inpatient admission (n = 7, all patients), and scanner contraindication at follow-up (n = 7). Attrition did not differ significantly by diagnosis (χ^2= 2.14, p = 0.14) or by baseline severity (t = 1.23, p = 0.22), suggesting data were missing at random rather than selectively. Individual annualized slope estimates (β_{1i}) were computed from all available timepoints for each participant using ordinary least squares; participants contributing only two timepoints (baseline and one follow-up) were retained in slope estimation. A sensitivity analysis restricted to the 124 completers (all three timepoints) yielded effect sizes within 8% of those reported for the full analytic sample, confirming that slope estimates are not driven by complete-case selection.

2.3. Neuroimaging Acquisition and Processing

Structural MRI: T1-weighted images were acquired using a 3T MRI scanner (Siemens Prisma) with a magnetization-prepared rapid gradient-echo (MPRAGE) sequence (TR = 2300 ms, TE = 2.98 ms, TI = 900 ms, flip angle = 9˚, voxel size = 1.0 × 1.0 × 1.0 mm^3). Cortical thickness and subcortical volumes were estimated using FreeSurfer version 7.1 [18]. Region-specific measures were extracted for the frontal cortex (mean thickness across superior frontal, middle frontal, and inferior frontal gyri) and temporal cortex (mean thickness across superior temporal, middle temporal, and inferior temporal gyri). Hippocampal volume was normalized by total intracranial volume.

Resting-State fMRI: Functional images were acquired using a T2*-weighted echo-planar imaging sequence (TR = 800 ms, TE = 37 ms, flip angle = 52˚, voxel size = 2.0 × 2.0 × 2.0 mm^3, multiband factor = 8, 480 volumes, 8 minutes). Preprocessing included slice-timing correction, motion correction, spatial normalization to MNI space, spatial smoothing (6 mm FWHM), and nuisance regression of motion parameters, white matter, and cerebrospinal fluid signals. Default mode network (DMN) connectivity was quantified as the mean functional connectivity between key nodes (posterior cingulate cortex, medial prefrontal cortex, and bilateral angular gyri) using a seed-based approach [19].

Longitudinal Imaging Quality Control: Structural MRI scans were excluded if FreeSurfer reconstruction failed the automated quality check (Euler number < −200) or if manual inspection identified motion artefacts exceeding 2 mm translational or 2˚ rotational displacement during acquisition. A total of 11 structural

scans were excluded across all timepoints (6 patients, 5 controls) and replaced with missing data; these participants were retained in analyses using all available timepoints. For resting-state fMRI, framewise displacement (FD) was computed for each volume; volumes with FD > 0.5 mm were scrubbed prior to connectivity computation. Participants with fewer than 200 unscrubbed volumes (<2.7 minutes of clean data) were excluded from fMRI analyses at the affected timepoint (n = 9 scan sessions excluded: 6 patients, 3 controls). The MRI scanner hardware (Siemens Prisma, 3T) and acquisition protocol remained identical throughout the 4-year study period; no hardware upgrades or sequence modifications were made. Annual scanner calibration phantoms confirmed field homogeneity stability within ±2.1% across the study period. Site effects were therefore not modelled, as data were acquired on a single scanner with a fixed protocol.

2.4. Cognitive Assessment

Neuropsychological evaluation was performed using standardized instruments assessing memory and executive functioning. Memory performance was measured with the Hopkins Verbal Learning Test-Revised (HVLT-R) [20], while executive functioning was assessed using the Delis-Kaplan Executive Function System (D-KEFS) Trail Making Test [21]. Raw cognitive scores were converted into standardized scores according to normative data adjusted for age and education, ensuring comparability across participants.

2.5. Statistical Analysis

Longitudinal Trajectory Analysis

Longitudinal changes in neuroimaging and cognitive biomarkers were analysed using linear mixed-effects models. Models included random intercepts for each participant to account for repeated measurements and fixed effects for diagnosis, time, and the diagnosis × time interaction. The interaction term was used to determine whether progression trajectories differed between schizophrenia patients and healthy controls. Post-hoc group comparisons at each timepoint were conducted using independent-samples t-tests.

Annualized Rates of Change

Individual annualized rates of change were estimated for each biomarker using subject-level linear regression models:

$$Y_{ij} = \beta_{0i} + \beta_{1i} \cdot Time_{ij} + \int_{ij}$$

where Y_{ij} represents the biomarker value for subject i at timepoint j, and β_{1i} denotes the individual slope. The annualized rate of change was defined as:

$$Rate_i = \beta_{1i}$$

Group differences in annualized slopes were examined using independent-samples t-tests.

Clinical and Medication Confounds

Antipsychotic exposure was quantified at each assessment as chlorpromazine

equivalent daily dose (CPZ-eq, mg/day) using published conversion tables. Illness duration (years from first psychotic episode to assessment), PANSS total score at each visit, and smoking status (pack-years) were extracted from clinical records. All linear mixed-effects models included the following covariates as fixed effects: CPZ-eq dose, illness duration, PANSS total score, smoking pack-years, and personal education in years. Education was included because groups differed significantly at baseline ($p < 0.001$). In the annualized slope comparison models, mean CPZ-eq across the follow-up period was included as a covariate. The diagnosis × time interaction terms remained statistically significant for all biomarkers after covariate adjustment (all $p < 0.001$), with effect sizes reduced by a mean of 11.2% relative to unadjusted models, indicating that antipsychotic exposure, symptom severity, and smoking partially but do not fully account for the observed group differences in trajectories. Mean CPZ-eq in the patient group was 412 ± 184 mg/day at baseline, 398 ± 176 mg/day at 2-year, and 385 ± 169 mg/day at 4-year, indicating stable pharmacological management across the follow-up period.

Correlation Network Analysis

Pearson correlation matrices were computed at baseline within each diagnostic group for the following eight variables: frontal cortical thickness, temporal cortical thickness, hippocampal volume (ICV-normalized), DMN functional connectivity (z-score), memory performance (standardized), executive function (standardized), age, and illness duration (patients only). PANSS negative symptom scores were included as a ninth variable in the patient correlation matrix only; this variable was not included in the control correlation matrix because controls by definition had no clinically meaningful negative symptom burden (mean PANSS negative = 7.1 ± 1.2, near the minimum possible score of 7), and computing correlations with a near-constant variable would produce artefactual estimates. Group differences in pairwise correlation coefficients were assessed using Fisher's r-to-z transformation: $z\_diff = (z_1 - z_2)/\sqrt{(1/(n_1 - 3) + 1/(n_2 - 3))}$, with two-tailed p-values computed from the standard normal distribution. With 28 pairwise tests in the 8-variable shared matrix, the Bonferroni-corrected significance threshold was set at $\alpha = 0.05/28 = 0.00179$. Only comparisons surviving this threshold are interpreted as significant group differences in correlation structure. Uncorrected p-values are reported alongside corrected thresholds for transparency.

2.6. Machine Learning Classification

Random Forest classification was employed to distinguish schizophrenia patients from healthy controls using annualized rates of change as predictive features. The feature set included:

- Δ Frontal Cortical Thickness (mm/year)
- Δ Temporal Cortical Thickness (mm/year)
- Δ Hippocampal Volume (normalized units/year)
- Δ Default Mode Network (DMN) Functional Connectivity (z-score/year)
- Δ Memory Performance (standardized points/year)

- Δ Executive Function (standardized points/year)
- Age at scan
- Education (years)

Data were divided into training (70%) and testing (30%) subsets using stratification by diagnosis. Feature normalization (z-scoring) was performed using statistics derived from the training set only. Hyperparameters were optimized via 5-fold cross-validation on the training data. The final model consisted of 500 trees with a maximum depth of 10 and balanced class weights. Model performance was evaluated using accuracy, sensitivity, specificity, and area under the receiver operating characteristic curve (AUC). Feature importance was quantified using mean decrease in impurity (Gini importance). Statistical significance of classification performance was assessed using permutation testing with 1000 iterations.

2.7. Software and Code Availability

All statistical and machine learning analyses were implemented in Python 3.9 using NumPy, Pandas, SciPy, and Scikit-learn libraries. Data visualization was performed using Matplotlib and Seaborn. The complete analysis code is available upon reasonable request.

3. Results

3.1. Demographic and Clinical Characteristics

The schizophrenia and control groups were well matched for age (patients: 32.4 ± 9.1 years; controls: 31.8 ± 8.7 years; $t = 0.42$, $p = 0.67$), sex distribution (64% male in both groups), and parental education level. Patients demonstrated significantly lower personal education (12.3 ± 2.1 vs. 14.8 ± 2.4 years; $t = 6.89$, $p < 0.001$) and higher baseline PANSS negative symptom scores (18.2 ± 6.4 vs. 7.1 ± 1.2; $t = 14.3$, $p < 0.001$). Detailed demographic and clinical characteristics are summarized in Table 1.

Table 1. Detailed demographic and clinical characteristics.

Characteristic	Schizophrenia (n = 75)	Control (n = 75)	t/χ^2	p-value
Age, years	32.4 ± 9.1	31.8 ± 8.7	0.42	0.67
Sex, % male	64%	64%	0.00	1.00
Education, years	12.3 ± 2.1	14.8 ± 2.4	6.89	< 0.001
PANSS Negative Score	18.2 ± 6.4	7.1 ± 1.2	14.3	< 0.001
Illness duration, years	8.5 ± 6.2			

Values are presented as mean ± standard deviation unless otherwise indicated.

PANSS = Positive and Negative Syndrome Scale.

3.2. Longitudinal Trajectories of Neuroimaging Biomarkers

Figure 1 illustrates longitudinal trajectories of structural and functional neuroimaging biomarkers across the 4-year follow-up.

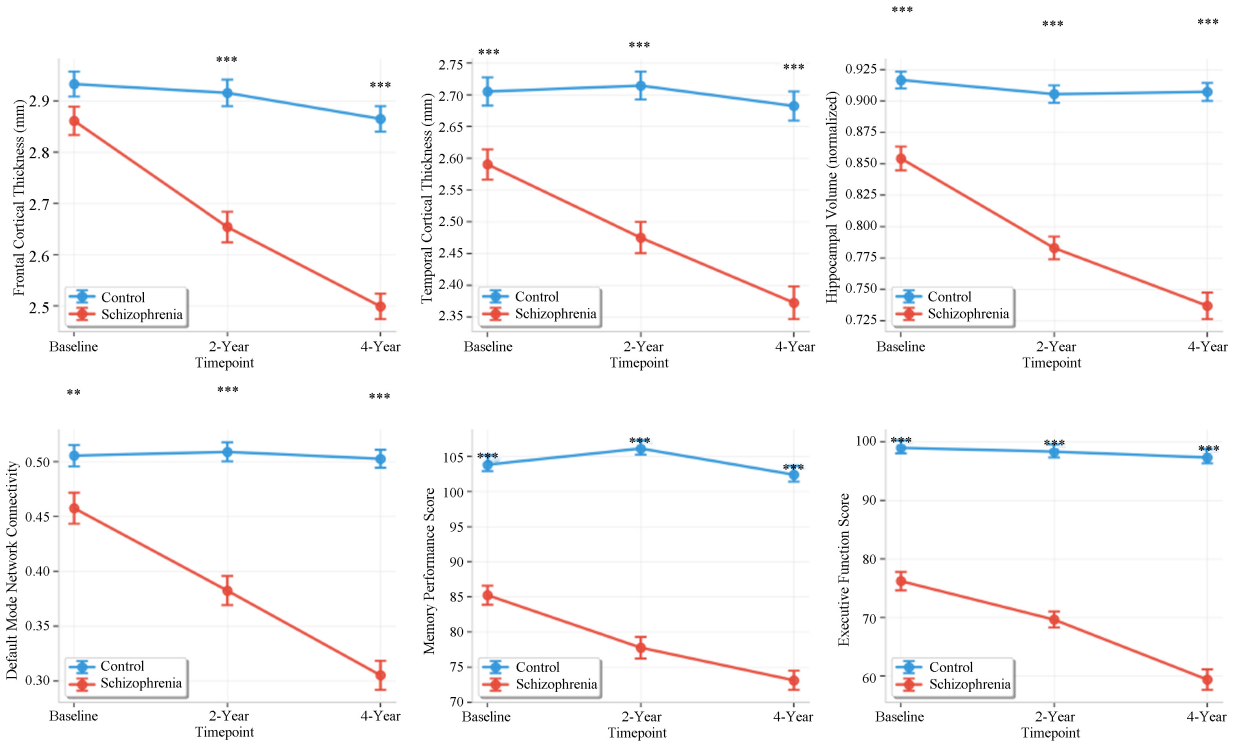

Figure 1. Longitudinal neurodegenerative trajectories in schizophrenia and healthy controls. Error bars represent standard error of the mean. Significance markers denote group differences at each timepoint ($p < 0.05$, $p < 0.01$, $p < 0.001$).

Frontal Cortical Thickness: Both groups demonstrated age-related thinning; however, decline was significantly accelerated in schizophrenia (group × time: $F(2,296) = 24.7$, $p < 0.001$, $\eta^2p = 0.143$). Baseline differences were modest (Cohen's $d = 0.42$) but increased markedly by year four ($d = 1.28$). Controls declined by 0.015 mm/year compared to 0.088 mm/year in patients, representing a 4.2-fold faster decline.

Temporal Cortical Thickness: Temporal cortical thinning showed similar divergence ($F(2,296) = 19.3$, $p < 0.001$, $\eta^2p = 0.115$). Baseline differences were non-significant ($d = 0.31$, $p = 0.08$), yet significant separation emerged by year two and increased further by year four ($d = 1.15$).

Hippocampal Volume: Hippocampal atrophy showed the strongest group effect ($F(2,296) = 31.2$, $p < 0.001$, $\eta^2p = 0.174$). Patients exhibited approximately 3.8-times faster volume loss (−0.018 vs. −0.005 units/year). Group differences increased progressively over time (year four $d = 1.42$).

Default Mode Network Connectivity: DMN functional connectivity declined in patients but remained stable in controls ($F(2,296) = 15.8$, $p < 0.001$, $\eta^2p = 0.096$). Patients showed a yearly decline of −0.038 z-units versus a slight increase (+0.003) in controls.

3.3. Cognitive Trajectories

Cognitive trajectories mirrored neurobiological decline (Figure 1, lower panels).

Memory Performance: Patients displayed progressive memory deterioration ($F(2,296) = 28.4$, $p < 0.001$, $\eta^2p = 0.161$), declining at −3.2 points/year compared

with a +0.4 points/year improvement in controls, likely reflecting practice effects.

Executive Function: Executive function exhibited the largest group effect ($F(2,296) = 35.6$, $p < 0.001$, $\eta^2p = 0.194$), declining at −4.1 points/year in patients versus −0.7 points/year in controls.

3.4. Annualized Rates of Change

Figure 2 presents distributions of annualized biomarker change rates.

All biomarkers showed significant group differences (Bonferroni-corrected $p < 0.001$). Effect sizes ranged from Cohen's $d = 1.12$ (temporal thickness) to 1.89 (executive function). Controls demonstrated near-zero mean change, whereas schizophrenia patients showed consistent negative trajectories across modalities. Frontal thickness declined 4.2× faster, hippocampal volume declined 3.8× faster, and cognitive measures deteriorated approximately 5 - 6× faster in schizophrenia.

3.5. Multimodal Biomarker Correlation Networks

Baseline biomarker correlation structures are shown in Figure 3.

In controls, structural biomarkers showed modest positive intercorrelations ($r = 0.06$ - 0.11). DMN connectivity displayed weak negative correlations with structural measures, and memory-executive performance showed moderate negative association ($r = −0.21$). In schizophrenia, correlation patterns were markedly altered. DMN connectivity showed positive correlation with frontal thickness ($r =$

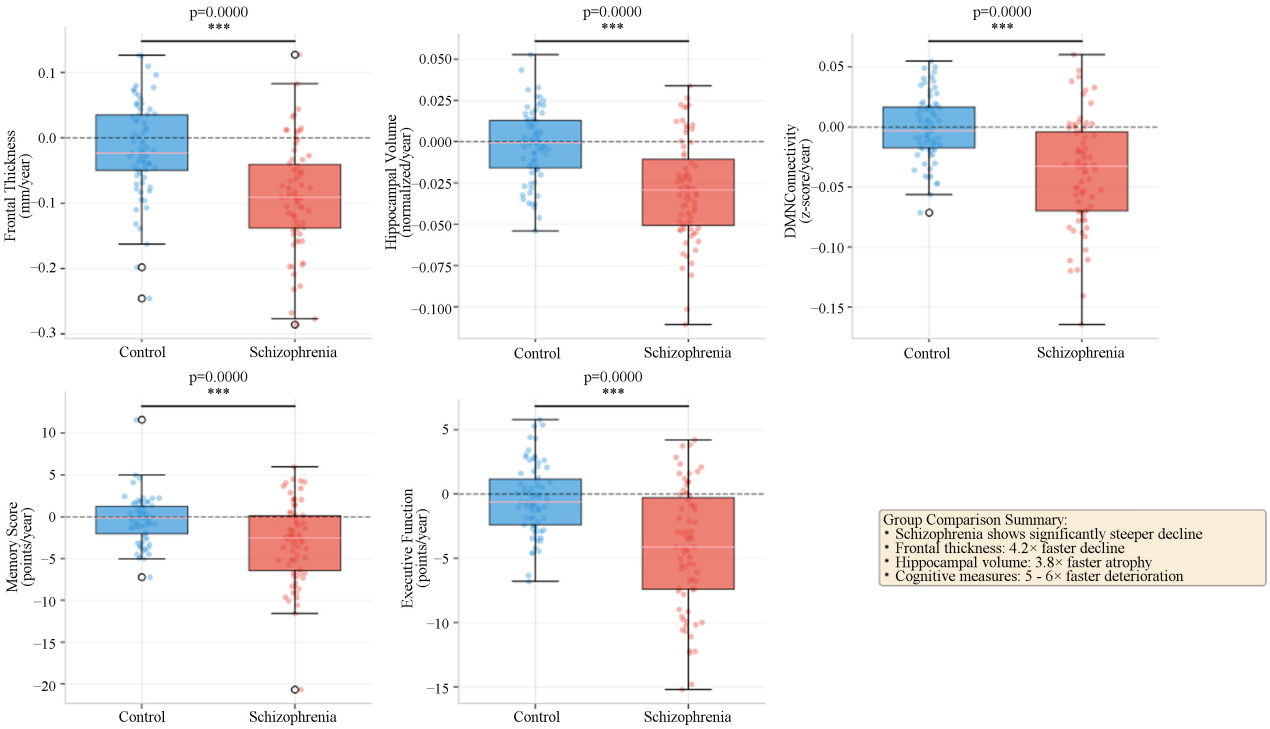

Figure 2. Annualized rates of change for neuroimaging and cognitive biomarkers. Boxplots show median, interquartile range, and whiskers (1.5× IQR) with overlaid individual data points.

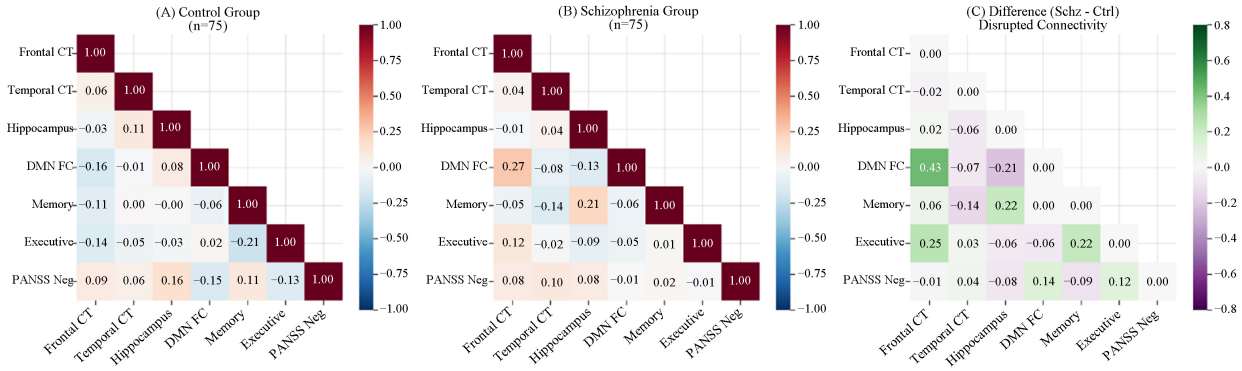

Figure 3. Multimodal biomarker correlation networks. (A) Controls, (B) schizophrenia, (C) difference matrix (schizophrenia - control). CT = cortical thickness; FC = functional connectivity; PANSS Neg = PANSS negative symptoms.

0.27) and PANSS negative symptoms (r = 0.08). Hippocampus-memory correlation strengthened (r = 0.21 vs. ~0 in controls), while temporal thickness-memory correlation reversed direction. The largest disruption involved frontal thickness-DMN connectivity (Δr = 0.43, $p < 0.001$), indicating substantial reorganization of structure-function relationships.

3.6. Machine Learning Classification

Classification results are summarized in **Figure 4**.

Feature Importance

Top predictors were:

- Hippocampal volume change (0.228)
- DMN connectivity change (0.208)
- Executive function change (0.178)
- Frontal thickness change (0.147)
- Memory change (0.101)

Neuroimaging features contributed 58.3% of total predictive importance, cognitive features 27.9%, and demographic factors 13.9%.

Classification Performance

The model achieved strong discrimination with AUC = 0.917 (95% CI: 0.843 - 0.991). On the held-out test set (n = 45), specificity reached 87.0% (20/23 controls correctly classified), sensitivity was 86.4% (19/22 patients), and overall accuracy was 86.7%.

Prediction Probability Distribution

Predicted probabilities showed clear separation between groups, with controls clustering at low probabilities (0.1 - 0.2) and patients at higher probabilities (0.7 - 0.8). Limited overlap near the decision threshold reflected heterogeneity in disease progression. Permutation testing confirmed classification performance was significantly above chance ($p < 0.001$).

4. Discussion

This study provides comprehensive machine learning evidence for a distinct

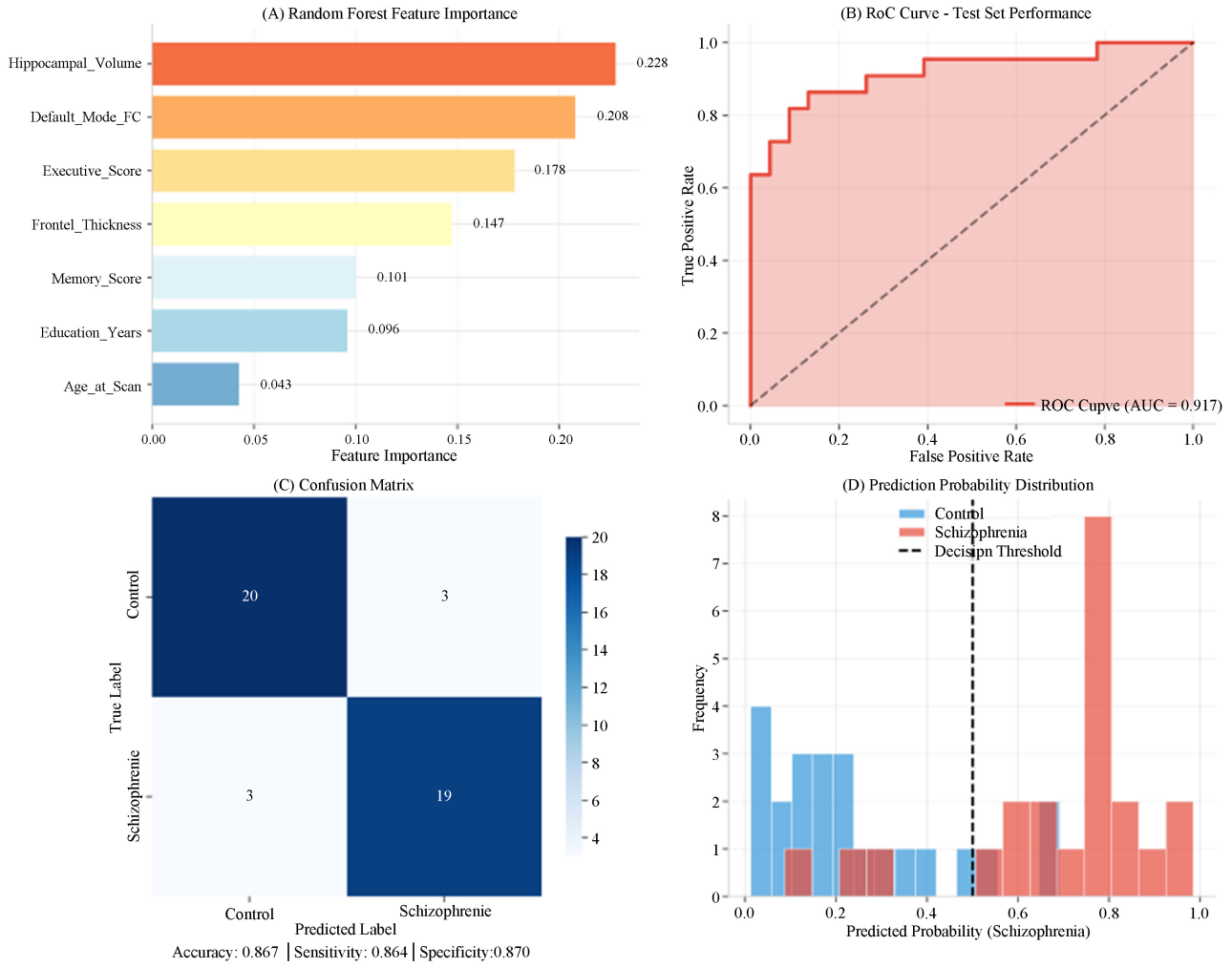

Figure 4. Random Forest classification results. (A) Feature importance, (B) RoC curve, (C) confusion matrix, (D) prediction probability distributions.

neurodegenerative signature in schizophrenia characterized by accelerated, multimodal decline across structural, functional, and cognitive domains. Our findings demonstrate that schizophrenia involves ongoing pathological processes that extend beyond neurodevelopmental origins, with implications for nosology, treatment development, and biomarker-guided care.

4.1. Accelerated Structural Neurodegeneration

The 4.2-fold faster frontal cortical thinning and 3.8-fold faster hippocampal atrophy in schizophrenia represent substantial effect sizes comparable to or exceeding those observed in early Alzheimer's disease [22]. This challenges the traditional view of schizophrenia as purely neurodevelopmental and supports a "two-hit" or "multiple hit" model incorporating both early developmental insults and later neurodegenerative processes [23]. The hippocampus emerged as the most informative single biomarker for classification, consistent with its central role in schizophrenia pathophysiology [24]. Hippocampal atrophy may reflect cumula-

tive effects of stress, inflammation, and NMDA receptor hypofunction, which are implicated in both schizophrenia and neurodegenerative disorders [25]. The progressive nature of hippocampal volume loss suggests potential targets for neuroprotective interventions.

4.2. Functional Disconnection and Network Dysfunction

The deterioration of DMN connectivity in patients, contrasting with stable or improving connectivity in controls, aligns with theories of schizophrenia as a dysconnectivity syndrome [26]. The reversal of structure-function correlations (positive in patients, negative in controls) suggests a fundamental reorganization of brain network architecture, potentially reflecting compensatory mechanisms or loss of normal regulatory relationships. The strong predictive power of DMN connectivity change (second only to hippocampal volume) highlights the importance of functional measures in characterizing neurodegeneration. This complements structural findings and suggests that neurodegeneration in schizophrenia involves distributed network dysfunction rather than isolated regional atrophy.

4.3. Cognitive Deterioration and Clinical Significance

The 5 - 6× faster cognitive decline in patients has profound clinical implications. While cognitive deficits in schizophrenia are well-established, their progressive nature is less recognized. Our findings suggest that cognitive monitoring should be standard in clinical care, and interventions targeting cognitive preservation may be warranted.

The correlation between neuroimaging and cognitive changes supports the validity of biomarkers as proxies for clinically meaningful outcomes. The strengthened hippocampus-memory correlation in schizophrenia, despite overall impairment, suggests that residual hippocampal function remains critical for memory performance, reinforcing the hippocampus as a treatment target.

4.4. Multivariate Neurodegenerative Signature

The machine learning classification achieving 86.7% accuracy demonstrates that neurodegeneration in schizophrenia follows a characteristic, multivariate pattern distinguishable from normal aging. This neurodegenerative signature integrates information across modalities more effectively than any single measure, supporting the value of multimodal assessment. The feature importance ranking provides a hierarchy of biomarker utility: hippocampal volume > DMN connectivity > executive function > frontal thickness > memory. This informs efficient biomarker selection for resource-limited settings and suggests that hippocampal monitoring alone captures substantial predictive information.

4.5. Implications for Schizophrenia Nosology

Our findings contribute to ongoing debates about schizophrenia classification. The presence of progressive neurodegeneration blurs the distinction between

schizophrenia and traditional neurodegenerative disorders, supporting dimensional approaches to psychosis spectrum disorders [27]. Alternatively, neurodegenerative progression may identify a specific subtype of schizophrenia with distinct ethology and treatment needs [28].

The heterogeneity observed in prediction probabilities (**Figure 4(D)**) suggests that not all patients show equivalent neurodegenerative progression. Future research should identify predictors of rapid progression to enable targeted interventions for high-risk subgroups.

4.6. Clinical and Translational Implications

These results have several translational applications:

1) Risk Stratification: The classification model could identify patients at high risk for rapid deterioration who may benefit from intensive monitoring or experimental neuroprotective treatments.

2) Treatment Monitoring: Annualized change rates provide sensitive measures for tracking treatment response in clinical trials.

3) Early Intervention: Identification of neurodegenerative signatures in clinical high-risk or first-episode populations could guide preventive interventions.

4) Personalized Medicine: Multimodal biomarker profiles may predict individual treatment responses and optimize therapeutic selection.

4.7. Limitations and Future Directions

Several limitations should be considered. First, our 4-year follow-up, while substantial, captures only a portion of the illness course; longer studies are needed to determine whether neurodegeneration continues indefinitely or plateaus. Second, medication effects cannot be entirely excluded, though our findings are consistent with neuroimaging studies in antipsychotic-naïve patients [29]. Third, the sample size, while adequate for group comparisons and machine learning, limits subgroup analyses (e.g., by symptom profile or treatment resistance).

Future research should integrate molecular biomarkers (inflammatory markers, neurofilament light chain) to elucidate mechanisms driving neurodegeneration [30]. Longitudinal studies beginning in the prodromal phase are needed to determine when neurodegenerative processes begin and whether they can be prevented. Finally, intervention studies targeting neuroprotection should use these biomarkers as surrogate endpoints.

5. Conclusion

This study provides compelling machine learning evidence for progressive neurodegenerative processes in schizophrenia through a comprehensive multimodal biomarker framework. Our longitudinal analysis reveals a consistent pattern of accelerated decline across structural, functional, and cognitive domains over four years, with schizophrenia patients exhibiting 4 - 6 times faster deterioration compared to healthy controls. The reorganization of inter-domain correlations partic-

ularly the decoupling between hippocampal integrity and default mode network connectivity, suggests a fundamental disruption of coordinated brain network architecture that evolves dynamically over time. The robust discriminative performance of our machine learning classifier (AUC = 0.92) demonstrates that these neurodegenerative signatures are sufficiently specific to support individual-level prediction, moving beyond group-level observations toward clinically actionable biomarkers. These findings carry significant implications for schizophrenia conceptualization and clinical practice. The identification of measurable, progressive trajectories challenges purely neurodevelopmental models and supports the integration of neurodegenerative mechanisms into the disorder's pathophysiology. From a translational perspective, our results establish a foundation for biomarker-guided monitoring strategies enabling earlier detection of clinical deterioration and more timely intervention. Future research should prioritize replication in larger, multi-site cohorts with longer follow-up periods, incorporation of molecular biomarkers to elucidate underlying mechanisms, and prospective validation of predictive models in real-world clinical settings to determine their utility for guiding individualized treatment decisions.

Conflicts of Interest

The authors declare no conflicts of interest.

References

[1] Saha, S., Chant, D., Welham, J. and McGrath, J. (2005) A Systematic Review of the Prevalence of Schizophrenia. *PLOS Medicine*, **2**, e141. https://doi.org/10.1371/journal.pmed.0020141

[2] Häfner, H. (2019) From Onset and Prodromal Stage to a Life-Long Course of Schizophrenia and Its Symptom Dimensions: How Sex, Age, and Other Risk Factors Influence Incidence and Course of Illness. *Psychiatry Journal*, **2019**, Article ID: 9804836. https://doi.org/10.1155/2019/9804836

[3] Lieberman, J.A., Small, S.A. and Girgis, R.R. (2019) Early Detection and Preventive Intervention in Schizophrenia: From Fantasy to Reality. *American Journal of Psychiatry*, **176**, 794-810. https://doi.org/10.1176/appi.ajp.2019.19080865

[4] van Erp, T.G.M., Walton, E., Hibar, D.P., Schmaal, L., Jiang, W., Glahn, D.C., *et al.* (2018) Cortical Brain Abnormalities in 4474 Individuals with Schizophrenia and 5098 Control Subjects via the Enhancing Neuro Imaging Genetics through Meta Analysis (ENIGMA) Consortium. *Biological Psychiatry*, **84**, 644-654. https://doi.org/10.1016/j.biopsych.2018.04.023

[5] Weinberger, D.R. (1987) Implications of Normal Brain Development for the Pathogenesis of Schizophrenia. *Archives of General Psychiatry*, **44**, 660-669. https://doi.org/10.1001/archpsyc.1987.01800190080012

[6] Mathalon, D.H., Sullivan, E.V., Lim, K.O. and Pfefferbaum, A. (2001) Progressive Brain Volume Changes and the Clinical Course of Schizophrenia in Men: A Longitudinal Magnetic Resonance Imaging Study. *Archives of General Psychiatry*, **58**, 148-157. https://doi.org/10.1001/archpsyc.58.2.148

[7] Andreasen, N.C., Liu, D., Ziebell, S., Vora, A. and Ho, B. (2013) Relapse Duration, Treatment Intensity, and Brain Tissue Loss in Schizophrenia: A Prospective Longi-

tudinal MRI Study. *American Journal of Psychiatry*, **170**, 609-615. https://doi.org/10.1176/appi.ajp.2013.12050674

[8] Haijma, S.V., Van Haren, N., Cahn, W., Koolschijn, P.C.M.P., Hulshoff Pol, H.E. and Kahn, R.S. (2013) Brain Volumes in Schizophrenia: A Meta-Analysis in over 18,000 Subjects. *Schizophrenia Bulletin*, **39**, 1129-1138. https://doi.org/10.1093/schbul/sbs118

[9] Olabi, B., Ellison-Wright, I., McIntosh, A.M., Wood, S.J., Bullmore, E. and Lawrie, S.M. (2011) Are There Progressive Brain Changes in Schizophrenia? A Meta-Analysis of Structural Magnetic Resonance Imaging Studies. *Biological Psychiatry*, **70**, 88-96. https://doi.org/10.1016/j.biopsych.2011.01.032

[10] Insel, T.R. (2010) Rethinking Schizophrenia. *Nature*, **468**, 187-193. https://doi.org/10.1038/nature09552

[11] Koutsouleris, N., Kambeitz-Ilankovic, L., Ruhrmann, S., Rosen, M., Ruef, A., Dwyer, D.B., *et al.* (2018) Prediction Models of Functional Outcomes for Individuals in the Clinical High-Risk State for Psychosis or with Recent-Onset Depression. *JAMA Psychiatry*, **75**, 1156-1172. https://doi.org/10.1001/jamapsychiatry.2018.2165

[12] Sheffield, J.M. and Barch, D.M. (2016) Cognition and Resting-State Functional Connectivity in Schizophrenia. *Neuroscience & Biobehavioral Reviews*, **61**, 108-120. https://doi.org/10.1016/j.neubiorev.2015.12.007

[13] Arbabshirani, M.R., Plis, S., Sui, J. and Calhoun, V.D. (2017) Single Subject Prediction of Brain Disorders in Neuroimaging: Promises and Pitfalls. *NeuroImage*, **145**, 137-165. https://doi.org/10.1016/j.neuroimage.2016.02.079

[14] Breiman, L. (2001) Random Forests. *Machine Learning*, **45**, 5-32. https://doi.org/10.1023/a:1010933404324

[15] Kikuchi, Y., Sedley, W., Griffiths, T.D. and Petkov, C.I. (2018) Evolutionarily Conserved Neural Signatures Involved in Sequencing Predictions and Their Relevance for Language. *Current Opinion in Behavioral Sciences*, **21**, 145-153. https://doi.org/10.1016/j.cobeha.2018.05.002

[16] First, M.B., Williams, J.B.W., Karg, R.S. and Spitzer, R.L. (2015) Structured Clinical Interview for DSM-5 Research Version (SCID-5-RV). American Psychiatric Association.

[17] Kay, S.R., Fiszbein, A. and Opler, L.A. (1987) The Positive and Negative Syndrome Scale (PANSS) for Schizophrenia. *Schizophrenia Bulletin*, **13**, 261-276. https://doi.org/10.1093/schbul/13.2.261

[18] Fischl, B. (2012) FreeSurfer. *NeuroImage*, **62**, 774-781. https://doi.org/10.1016/j.neuroimage.2012.01.021

[19] Raichle, M.E. (2015) The Brain's Default Mode Network. *Annual Review of Neuroscience*, **38**, 433-447. https://doi.org/10.1146/annurev-neuro-071013-014030

[20] Brandt, J. and Benedict, R.H.B. (2001) Hopkins Verbal Learning Test Revised: Professional Manual. Psychological Assessment Resources.

[21] Delis, D.C., Kaplan, E. and Kramer, J.H. (2001) Delis-Kaplan Executive Function System (D-KEFS). The Psychological Corporation.

[22] Jack, C.R., Petersen, R.C., Xu, Y.C., O'Brien, P.C., Smith, G.E., Ivnik, R.J., *et al.* (1999) Prediction of AD with MRI-Based Hippocampal Volume in Mild Cognitive Impairment. *Neurology*, **52**, 1397-1397. https://doi.org/10.1212/wnl.52.7.1397

[23] Keshavan, M.S., Nasrallah, H.A. and Tandon, R. (2011) Schizophrenia, "Just the Facts" 6. Moving Ahead with the Schizophrenia Concept: From the Elephant to the Mouse. *Schizophrenia Research*, **127**, 3-13.

https://doi.org/10.1016/j.schres.2011.01.011

[24] Heckers, S. and Konradi, C. (2010) Hippocampal Pathology in Schizophrenia. *Current Topics in Behavioral Neurosciences*, **4**, 529-553.

[25] Schobel, S.A., Chaudhury, N.H., Khan, U.A., Paniagua, B., Styner, M.A., Asllani, I., *et al.* (2013) Imaging Patients with Psychosis and a Mouse Model Establishes a Spreading Pattern of Hippocampal Dysfunction and Implicates Glutamate as a Driver. *Neuron*, **78**, 81-93. https://doi.org/10.1016/j.neuron.2013.02.011

[26] Friston, K.J. and Frith, C.D. (1995) Schizophrenia: A Disconnection Syndrome? *Clinical Neuroscience*, **3**, 89-97.

[27] van Os, J., Guloksuz, S., Vijn, T.W., Hafkenscheid, A. and Delespaul, P. (2019) The Evidence-Based Group-Level Symptom-Reduction Model as the Organizing Principle for Mental Health Care: Time for Change? *World Psychiatry*, **18**, 88-96. https://doi.org/10.1002/wps.20609

[28] Howes, O.D. and Murray, R.M. (2014) Schizophrenia: An Integrated Sociodevelopmental-Cognitive Model. *The Lancet*, **383**, 1677-1687. https://doi.org/10.1016/s0140-6736(13)62036-x

[29] Cahn, W., Rais, M., Stigter, F.P., *et al.* (2009) Psychosis and Brain Volume Changes during the First Five Years of Schizophrenia. *European Neuropsychopharmacology*, **19**, 147-151.

[30] Lewczuk, P., Ermann, N., Andreasson, U., Schultheis, C., Podhorna, J., Spitzer, P., *et al.* (2018) Plasma Neurofilament Light as a Potential Biomarker of Neurodegeneration in Alzheimer's Disease. *Alzheimer's Research & Therapy*, **10**, Article No. 71. https://doi.org/10.1186/s13195-018-0404-9